Structural And Thermal Profile of the Southern Sangre De Cristo Arch Between Sante Fe and Las Vegas, New Mexico, Tests the Style of Late Cretaceous-Paleogene Laramide Faulting in The Southern Rocky Mountains

Jacob O. Thacker

2025, pp. 153-164. https://doi.org/10.56577/FFC-75.153

in:

Geology of the Eastern San Juan Basin - Fall Field Conference 2025, Hobbs, Kevin M.; Mathis, Allyson; Van Der Werff, Brittney;, New Mexico Geological Society 75 th Annual Fall Field Conference Guidebook, 227 p. https://doi.org/10.56577/FFC-75

This page is intentionally left blank to maintain order of facing pages.

New Mexico Geological Society Guidebook, 75th Fall Field Conference, 2025, p. 153–164, https://doi.org/10.56577/FFC-75.153

STRUCTURAL AND THERMAL PROFILE OF THE SOUTHERN SANGRE DE CRISTO ARCH BETWEEN SANTE FE AND LAS VEGAS, NEW MEXICO, TESTS THE STYLE OF LATE CRETACEOUS–PALEOGENE LARAMIDE FAULTING IN THE SOUTHERN ROCKY MOUNTAINS

JACOB O. THACKER[1]

[1]Rocky Mountain College, 1511 Poly Drive, Billings, MT 59102; jacob.thacker@rocky.edu

Abstract—The style of strain accommodation on Late Cretaceous–Paleogene (Laramide) structures across the Colorado Plateau and Rocky Mountains is a longstanding debate. Evidence for strike-slip faulting has led some to suggest region-scale dextral strain in/from the Colorado Plateau, whereas others have found evidence for pervasive WSW–ENE horizontal shortening. In north-central New Mexico, these provinces merge across the San Juan Basin (Colorado Plateau) to the Nacimiento and Sangre de Cristo arches (Rocky Mountains). The Picuris-Pecos fault in the southern Sangre de Cristo arch exhibits evidence for strike-slip tectonism, but the timing of that tectonism may precede Late Cretaceous horizontal shortening. This study examines the arch system between Santa Fe and Las Vegas, New Mexico, to assess these opposing models. Two range-scale cross sections are presented to assess fault geometries and compiled apatite (U-Th)/He and fission-track thermochronology from across the range allow for a critique of arch kinematics. An imbricate fan geometry is proposed, whereby faults transition from steep reverse faults at the range crest to shallow thrusts at the range front. The resolution of thermochronology data is limited but appears to support an east-stepping progression of exhumation. These interpretations are consistent with horizontal shortening accommodated on an imbricate fan system that stepped eastward through time (in sequence). Thrusts are interpreted to root into a mid- to upper-crustal detachment that is postulated to connect with the Nacimiento arch as a backthrust to this system.

INTRODUCTION

The style and timing of Late Cretaceous–Paleogene Rocky Mountain and Colorado Plateau Laramide-style (thick-skinned, basement-involved) arches and accompanying basins are not fully understood. Early ideas on the style of strain invoked vertical and/or high-angle normal faults (e.g., Stearns, 1978), major strike-slip wrench tectonics (Sales, 1968), or horizontal shortening via reverse and thrust faults (Berg, 1962; Blackstone, 1980). Oil and gas exploration in the 1960s–1980s confirmed thrust and reverse fault geometries, lending credence to horizontal shortening. Since then, it has been shown that the Rocky Mountain and Colorado Plateau Laramide region likely accommodated pervasive WSW–ENE shortening (Bump and Davis, 2003; Bump 2004; Erslev and Koenig, 2009) and structural linkages between the Sevier (thin-skinned) and Laramide belts have been proposed (Parker and Pearson, 2023). At the local scale, mapping and analysis show that thin-skinned-style tectonics commonly accent thick-skinned structures (e.g., Geraghty, 2013; Gray et al., 2019).

The structural style of typic Laramide features in the Colorado Plateau and Rocky Mountains in Arizona, Utah, Colorado, and Wyoming has received extensive study (Bump and Davis, 2003; Bump 2004; Erslev and Koenig, 2009; Weil and Yonkee, 2023). However, Laramide features in New Mexico have garnered less attention. Northern New Mexico represents a nexus of two dominant Laramide styles (Karlstrom et al., 2024): Colorado Plateau (San Juan Basin) and Rocky Mountain (Nacimiento and Sangre de Cristo arches and Raton Basin). How these domains relate has been the topic of much debate, with some researchers considering the Colorado Plateau distinct from the Rocky Mountains (e.g., Chapin and Cather, 1981), whereas others have acknowledged the differences in deformation magnitude but consider Laramide structures across these provinces together as they relate to tectonic processes (e.g., Thacker et al., 2023). Both ideas elicit distinct interpretations on the style of strain accommodation.

In north-central New Mexico, two models for Laramide strain accommodation are presented: large-magnitude strike-slip tectonism, possibly as the result of a semidetached Colorado Plateau microplate and/or changing strain vectors over time (Karlstrom and Daniel, 1993; Bauer and Ralser, 1995; Cather, 1999; Cather, 2004; Cather et al., 2006), or horizontal shortening (Erslev, 2001; McDonald, 2003; Fankhauser and Erslev, 2004; Pollock et al., 2004) via a regionally pervasive WSW–ENE strain field. More specifically, the eastern San Juan Basin and Nacimiento arch and the western Sangre de Cristo arch are the focus of this debate. The controversy is exacerbated in that both locations show convincing evidence for horizontal shortening (Erslev, 2001; Fankhauser and Erslev, 2004; Pollock et al., 2004; Bailey et al., 2024) as well as geometrically viable observations for strike-slip tectonism (Woodward et al., 1992; Bauer and Ralser, 1995; Cather, 1999; Cather et al., 2006; Bailey et al., 2024).

The Sangre de Cristo arch (Fig. 1) represents an opportunity to test these end-member models. The Picuris-Pecos fault in

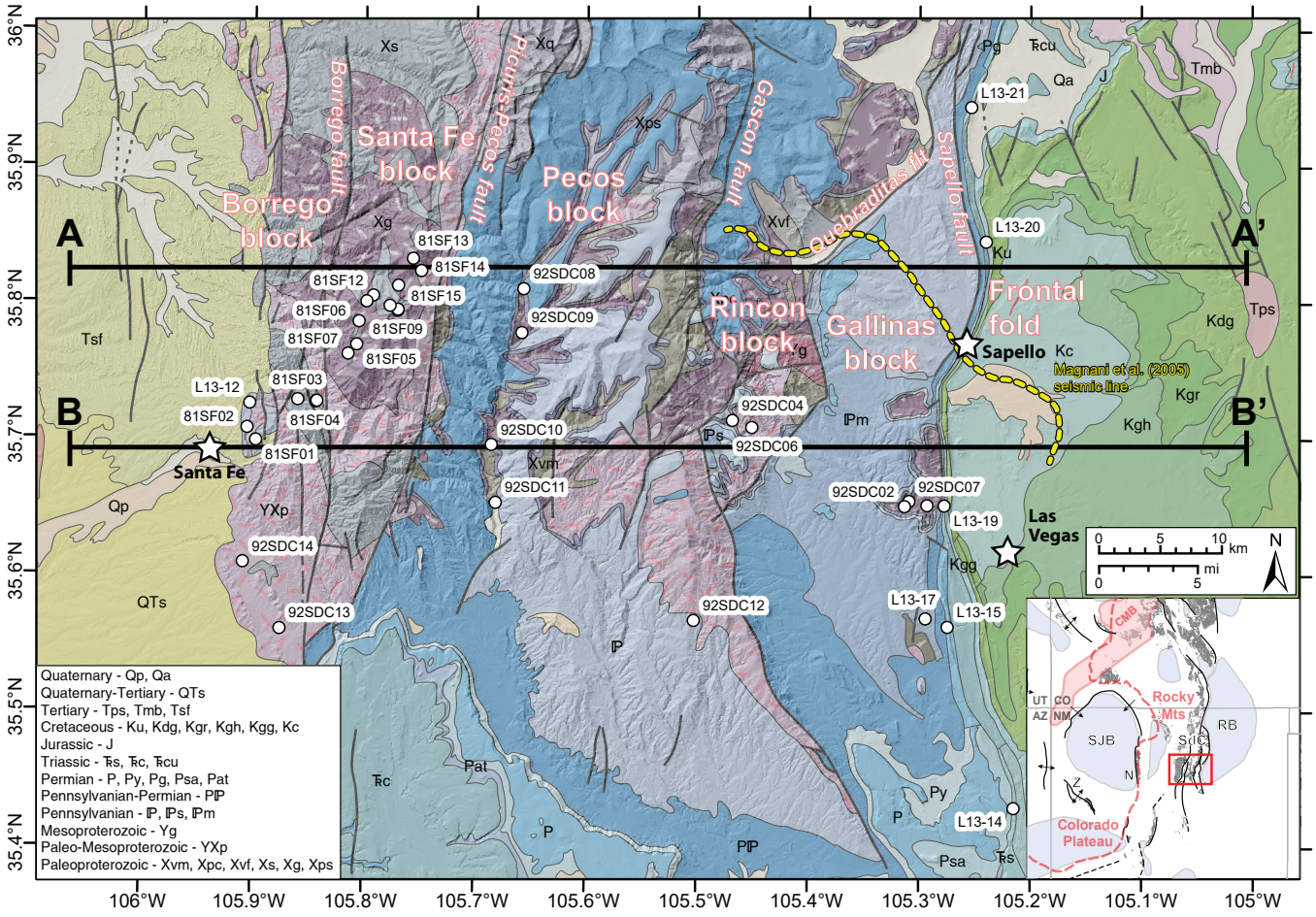

Figure 1. Geologic map of the southern Sangre de Cristo range between Santa Fe and Las Vegas, New Mexico. Map data and units are from Scholle (2003). Structural blocks that make up the Sangre de Cristo arch as discussed in the text and locations of compiled thermochronology data and the Magnani et al. (2005) seismic line location are shown. Cross-section lines A–A' and B–B' are presented in Figure 2. Inset map at bottom right shows Late Cretaceous–Paleogene Laramide-style structures in New Mexico and southern Colorado. SJB: San Juan Basin; RB: Raton Basin; SdC: Sangre de Cristo arch; N: Nacimiento arch; Z: Zuni arch; CMB: Colorado Mineral Belt.

the Sangre de Cristo arch has been pointed to as an example of both Laramide strike-slip tectonism (Bauer and Ralser, 1995; Cather et al., 2006) and horizontal shortening (Erslev, 2001; McDonald, 2003; Fankhauser and Erslev, 2004). The geometry of the arch exhibits discrete structural blocks bounded by reverse/thrust fault zones (Fig. 1). At present, mapping and geophysical datasets allow for detailed cross-section construction, and adequate thermochronology data exist across the arch. This study contributes two new range-scale cross sections of the southern Sangre de Cristo arch, while previously published apatite (U-Th)/He (AHe) and fission-track (AFT) data are leveraged to interpret the arch's kinematic history. From these results, the structural style of the region is considered, and possible connection to the Nacimiento arch through a mid-crustal detachment is proposed.

GEOLOGIC BACKGROUND

Laramide-style deformation in the western interior USA refers to thick-skinned, basement-involved structural arches formed via deep-seated reverse and thrust faults (Weil and Yonkee, 2023). Arches are accompanied by deeply subsided basins that acted as relatively small-wavelength (tens to hundreds of kilometers) depocenters for synorogenic deposition that compartmentalized the preexisting large-wavelength (hundreds to thousands of kilometers) retroarc foreland basin. Arches and basins display an anastomosing pattern (Woodward, 1976; Stone, 1986; Erslev, 1993) and formed >1000 km inboard of the Late Cretaceous–Paleogene convergent margin (e.g., Yonkee and Weil, 2015). The geometry and kinematics of Laramide features have been examined in detail across the Colorado Plateau (Bump and Davis, 2003; Bump, 2004; Davis and Bump, 2009) and Rocky Mountains (Woodward, 1976; Stone, 1986; Erslev, 1993; Erslev and Koenig, 2009; Weil and Yonkee, 2023). The main distinction between these two structural domains is that Colorado Plateau Laramide structures commonly exhibit ≤2 km structural relief, whereas structural relief on Rocky Mountain arches is commonly ≥2 km (Karlstrom et al., 2022).

The Sangre de Cristo arch between Santa Fe and Las Vegas, New Mexico, represents a Rocky Mountain-style structure, with structural relief from the range crest to Raton Basin floor on the order of 4.5–5.3 km. The Sangre de Cristo massif represents a continuous structural arch from south-central

Colorado to south of Santa Fe. The western part of the range exhibits normal faults associated with the Rio Grande rift (Koning and Read, 2010). At the latitude of Santa Fe, these faults dissect part of the former Laramide structure at the base of the Santa Fe Range but are opposite the major rift-bounding Pajarito fault near the town of Los Alamos. The Sangre de Cristo arch exhibits only minor Rio Grande rift faulting over the study area.

Discrete structural blocks bounded by fault zones (Figs. 1 and 2) make up the Sangre de Cristo arch. From west to east, these are defined herein as the Borrego block (Santa Fe range front to Borrego fault), Santa Fe block (Borrego fault, west, Picuris-Pecos fault, east), Pecos block (Picuris-Pecos fault, west, Gascon fault, east), Rincon block (Gascon fault, west, Hermit Peak and Quebraditas faults, east), and Gallinas block (Hermit Peak and Quebraditas faults, west, Sapello and Montezuma faults, east), and the frontal fold structural zone. In geographic terms, blocks represent the Santa Fe Range (Borrego and Santa Fe blocks), Pecos River area (Pecos block), and the Rincon Range (Rincon and Gallinas blocks), while the frontal fold contains the town of Sapello and is referred to as The Creston south of there. For the purpose of discussion, major fault systems are simplified as the Quebraditas system (Hermit Peak and Quebraditas faults) and the Sapello fault

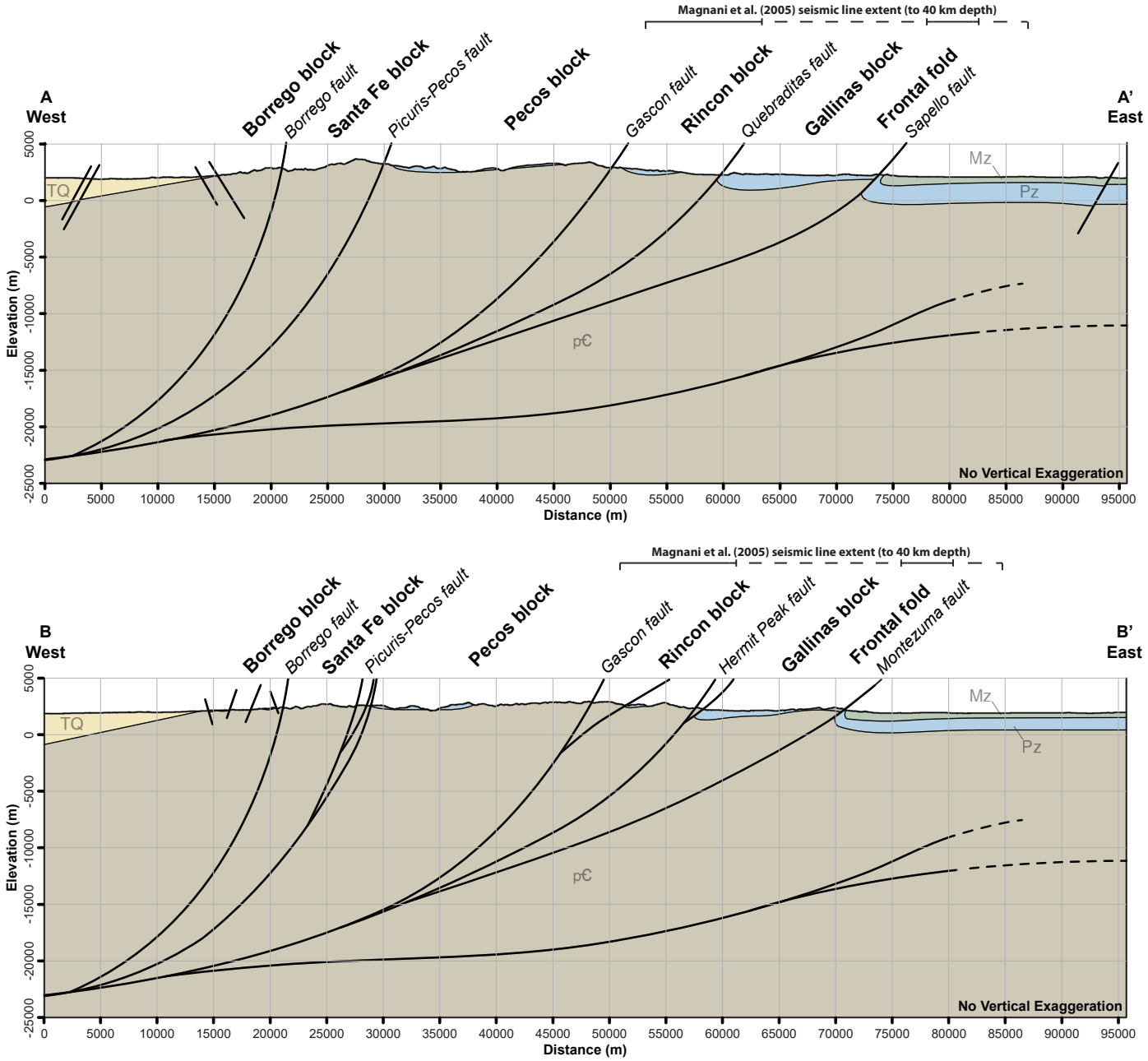

Figure 2. Unbalanced admissible trans-range cross sections; structural blocks and faults from Figure 1 and in text labeled. Extent of seismic data presented in Magnani et al. (2005) shown; dashed portions of line represent part of seismic section that was taken oblique to NNE–SSW structural grain at range front. pC = Proterozoic basement; Pz = Paleozoic strata; Mz = Mesozoic strata; TQ = Tertiary–Quaternary rift basin fill. A: Northern cross-section line A–A'. B: Southern cross-section line B–B'.

system (Sapello and Montezuma faults).

The Picuris-Pecos fault in the Sangre de Cristo arch has been pointed to as an example of Laramide strike-slip tectonism (Bauer and Ralser, 1995; Cather et al., 2006). Estimates suggest ~37 km of Late Cretaceous dextral slip on the fault (Chapin and Cather, 1981; Cather, 1999). The Sangre de Cristo arch has also been considered as a transpressive flower structure (Bauer and Ralser, 1995). Those in favor of horizontal shortening have presented evidence that strike-slip tectonism predated the Late Cretaceous, likely occurring during the Proterozoic (Fankhauser and Erslev, 2004). Horizontal shortening models do not disregard Laramide dextral slip, but rather suggest it was minimal (<5 km) and a product of oblique shortening (Erslev, 2001; McDonald, 2003) as WSW–ENE shortening was accommodated on an approximately N–S to NNE–SSW trending structural grain.

Previously published AFT and AHe thermochronology data exist from each structural block and the frontal fold. Kelley and Duncan (1986) presented AFT data from north-central New Mexico to examine Laramide to Rio Grande rift exhumation. Their Santa Fe Range (Borrego and Santa Fe blocks) data exclusively show Late Cretaceous–Eocene cooling that they attributed to Laramide tectonism (Kelley and Duncan, 1986; Kelley et al., 1992). Apatite fission-track thermochronology and AHe data from the Pecos River area and Rincon Range were reported by Landman (2016) to understand Cenozoic landscape evolution of the range. Samples from the central Pecos River area (Pecos and Rincon blocks) exhibited mid-Tertiary cooling, and were interpreted to represent exhumation due to Rio Grande rift extension. Samples from the eastern Rincon Range (Gallinas block and frontal fold) exhibited middle Miocene dates that Landman (2016) attributed to kilometer-scale unroofing to form the sub-Ogallala Formation unconformity.

METHODS

Two range-scale cross sections (Figs. 2A and 2B) were hand drafted at 1:250,000 scale then digitized in Adobe Illustrator. Geologic constraints for these sections were compiled from large- (1:24,000) to small-scale (1:500,000) geologic maps (Baltz, 1972; Baltz and Meyers, 1999; Lisenbee, 2003; Scholle, 2003; Koning and Read, 2010), cross sections (C–C', D–D', E–E', and F–F' in Baltz and Meyers, 1999), and geophysical data (Magnani et al., 2005). More specifically, surface locations for faults from the Borrego, Santa Fe, and Pecos blocks were constrained by small-scale mapping (Scholle, 2003), with subsurface expressions interpreted. Surface locations and subsurface expression of Rincon and Gallinas block faults and the frontal fold were constrained from moderate-scale (1:125,000; Baltz and Meyers, 1999) to large-scale (1:24,000; Baltz, 1972; Lisenbee, 2003) geologic maps, cross sections, and geophysical data from Magnani et al. (2005). Thicknesses for Pennsylvanian–Permian strata were constrained from mapping by Baltz and Meyers (1999). The cross sections are not balanced, but the eastern parts (Rincon Range) are constrained by seismic data from Magnani et al. (2005).

The thermal history of each block was examined via thermochronology under the premise that cooling was the result of erosion-driven exhumation from structural deformation. Apatite (U-Th)/He and AFT data (Table 1) were analyzed by examining dates (Figs. 3A–3C), AFT lengths (Fig. 3D), and AHe date-effective uranium (eU; eU = U + 0.235Th) patterns spatially against longitude and by structural location. Forward models were used to test hypothetical time-temperature histories against the date-eU patterns in the overall AHe dataset. Forward models were constructed in HeFTy (Ketcham, 2005) using the helium-diffusion kinetic model RDAAM (Flowers et al., 2009), a fission-track annealing resistance (R_{mr0}) value of 0.83, and a 47-μm grain radius based on the average radius calculated from the overall dataset (46.78 μm). Four grossly simplified hypothetical time-temperature paths were run against the data to explore potential exhumation histories from each structural location (Figs. 4 and 5).

In all forward models, time-temperature histories started at 20°C and were heated to 120°C; timing of maximum heating and onset of cooling were staggered in 10 My intervals from 85–55 Ma to test timing of exhumation. All models began at 300 Ma for Proterozoic-age samples to account for possible uplift during Ancestral Rocky Mountain deformation; Triassic-age samples from the frontal fold utilized a 200 Ma starting point, although the 120°C maximum heating is hot enough to reset all AHe dates (Wolf et al., 1998). Tested time-temperature histories represent single-stage cooling over 15 My (Fig. 4A) or 25 My (Fig. 4B) duration, and two-stage cooling episodes with an initial 15 My-duration cooling followed by slow cooling (Fig. 4C), and slow cooling followed by later rapid cooling (Fig. 4D).

RESULTS AND DISCUSSION

Structural Framework

Based on surface constraints, cross-section lines A–A' and B–B' show a shallowing of fault dips from west to east. The Borrego and Picuris-Pecos faults display steep, near-vertical faults (Sutherland, 1963; Bauer and Ralser, 1995) and faults toward the east display shallower dips to reverse and thrust faults. Mapping by Baltz and Meyers (1999) shows the Gascon fault system to represent a >45° reverse fault, the Quebraditas fault system as a <45° reverse/thrust fault, and the Sapello fault system as a >45° reverse fault. Along State Road 94, however, the surface trace of the Sapello fault represents a thrust geometry (fig. 64 of Baltz and Meyers, 1999) and is interpreted as <45° dip on the Figure 2 cross sections and according to seismic constraints (Magnani et al., 2005). Thickness variations in Paleozoic strata are evident from A–A' and B–B' (Fig. 2), as shown by Baltz and Meyers (1999). Assuming that the Quaternary–Proterozoic contact at the west end of each cross section is representative of the relict backlimb surface during the Late Cretaceous–Paleogene, it is evident that the west-rotated backlimbs of each block decrease eastward.

The style and depth to faulting for the eastern Quebraditas and Sapello faults are constrained by seismic reflection data

TABLE 1. Compiled Thermochronology Data

Structural Location	Sample	Elevation (m)	Latitude	Longitude	Rock	AHe	AFT	Reference
Borrego	81SF01	2256	35.698	−105.899	Proterozoic granite		x	1, 2
Borrego	81SF02	2296	35.708	−105.907	Proterozoic granite		x	1, 2
Borrego	81SF03	2421	35.728	−105.861	Proterozoic granite		x	1, 2
Borrego	81SF04	2488	35.727	−105.845	Proterozoic granite		x	1, 2
Borrego	92SDC13	2194	35.560	−105.876	Proterozoic granite	x	x	3
Borrego	92SDC14	2194	35.609	−105.910	Proterozoic granite	x	x	3
Borrego	81SF16	2524	35.727	−105.844	Proterozoic granite		x	1, 2
Borrego	L13-12	2226	35.725	−105.904	Proterozoic amphibolite	x		3
Santa Fe	81SF05	2985	35.769	−105.809	Proterozoic granite		x	1, 2
Santa Fe	81SF06	3128	35.786	−105.807	Proterozoic granite	x	x	1, 2, 3
Santa Fe	81SF07	2924	35.762	−105.816	Proterozoic granite	x	x	1, 2, 3
Santa Fe	81SF08	3732	35.795	−105.772	Proterozoic granite		x	1, 2
Santa Fe	81SF09	3744	35.794	−105.772	Proterozoic granite	x	x	1, 2, 3
Santa Fe	81SF10	3634	35.797	−105.779	Proterozoic granite		x	1, 2
Santa Fe	81SF11	3610	35.801	−105.800	Proterozoic granite		x	1, 2
Santa Fe	81SF12	3415	35.805	−105.794	Proterozoic granite	x	x	1, 2, 3
Santa Fe	81SF13	3848	35.832	−105.758	Proterozoic granite		x	1, 2
Santa Fe	81SF14	3543	35.823	−105.751	Proterozoic granite	x	x	1, 2, 3
Santa Fe	81SF15	3238	35.812	−105.771	Proterozoic granite		x	1, 2
Pecos	92SDC08	2482	35.810	−105.658	Proterozoic amphibolite	x	x	3
Pecos	92SDC09	2408	35.778	−105.660	Proterozoic metavolcanics		x	3
Pecos	92SDC10	2280	35.696	−105.687	Proterozoic trondhjemite	x	x	3
Pecos	92SDC11	2207	35.653	−105.683	Proterozoic granite	x	x	3
Rincon	92SDC04	2479	35.714	−105.470	Proterozoic granite		x	3
Rincon	92SDC06	2375	35.709	−105.452	Proterozoic biotite schist	x	x	3
Rincon	92SDC12	2582	35.567	−105.504	Proterozoic granite	x	x	3
Gallinas	92SDC01	2085	35.652	−105.294	Proterozoic granitic gneiss	x	x	3
Gallinas	92SDC02	2210	35.652	−105.315	Proterozoic granitic gneiss	x	x	3
Gallinas	92SDC07	2177	35.655	−105.311	Proterozoic granite		x	3
Gallinas	L13-17	2046	35.569	−105.296	Proterozoic granitic gneiss	x		3
Frontal Fold	L13-14	1844	35.430	−105.216	Triassic Santa Rose Fm. sandstone	x		3
Frontal Fold	L13-15	2009	35.563	−105.276	Triassic Santa Rose Fm. sandstone	x		3
Frontal Fold	L13-19	2053	35.652	−105.279	Triassic Santa Rose Fm. sandstone	x		3
Frontal Fold	L13-20	2191	35.846	−105.241	Triassic Chinle Group sandstone	x		3
Frontal Fold	L13-21	2136	35.945	−105.255	Triassic Santa Rose Fm. sandstone	x		3

Summary of compiled apatite (U-Th)/He (AHe) and apatite fission-track (AFT) data.
Detailed data are presented in Kelley and Duncan (1986); Kelley et al. (1992); and Landman (2016).
1 = Kelley and Duncan (1986)
2 = Kelley et al. (1992)
3 = Landman (2016)

by Magnani et al. (2005). Magnani et al. (2005) interpret these thrusts as 30° near the surface and to flatten to a 10° apparent dip at 5 km (Quebraditas) and 10 km (Sapello) depths. A deeper seismic reflector at 25 km depth is also noted by Magnani et al. (2005) that has parallelism with the Quebraditas and Sapello fault systems. They state that this feature appears to represent a Laramide detachment but rather interpret the feature as an older, inherited west-dipping crustal fabric. Herein, the interpretation is made instead that this feature does represent a Laramide detachment at depth (Fig. 2). The Magnani et al. (2005) seismic data shows the feature shallowing to the east to 10–15 km depth and splitting into two reflectors that remain flat for the remainder of their seismic line. A bend in this part of the seismic line to north-south causes the line to be approximately parallel to the NNE–SSW structural grain here, and it is interpreted herein that this would result in an approximately

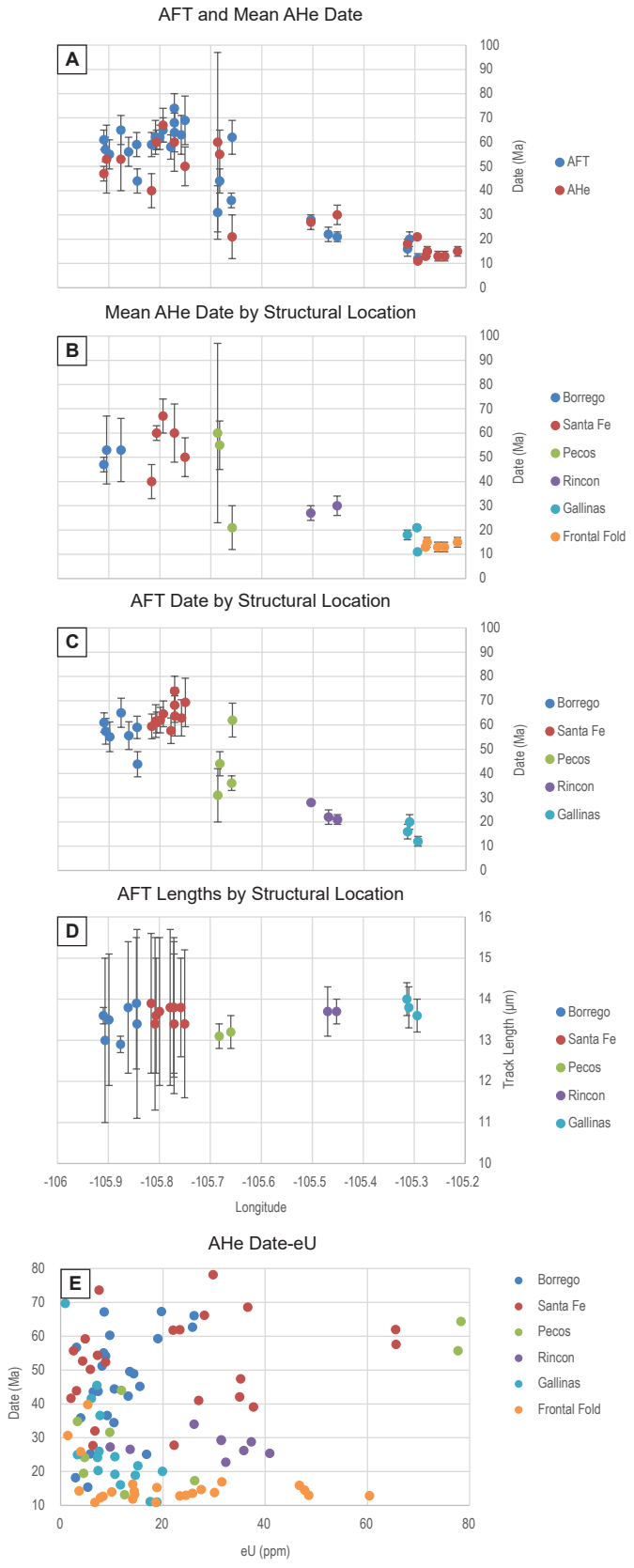

Figure 3. Thermochronology data by longitude (A–D) and AHe date-eU patterns (E). A: AFT and mean AHe dates. B: Mean AHe dates by structural location. C: AFT dates by structural location (blocks). D: AFT lengths by structural location. Note distinct date and track length patterns for each structural block. E: AHe date-eU patterns color-coded for structural location.

flat apparent dip for these reflectors. The interpretation in the east-west structural cross sections (Fig. 2) shows the upper reflector to die out east of the range front while the lower reflector is continuous.

The interpretation of these 10–15 km depth reflectors on the Figure 2 cross sections is tenuous. Termination of the upper reflector was interpreted based on subtle deformation above that feature in the Raton Basin (Las Vegas subbasin). Magnani et al. (2005) suggest that the reflection must predate Laramide deformation since the Raton Basin (Las Vegas subbasin) strata are undeformed. However, seismic profiles in their analysis (figs. 6 and 7 in Magnani et al., 2005) show slight deformation, and they note thinning of the Mesozoic strata to the southeast that would be consistent with synclinal bending and surface erosion of this strata. The regional geology shows considerable deformation to the Mesozoic strata here, as the synclinal low of the basin is coincident between Las Vegas to the south and northeast of Sapello (Fig. 1). This interpretation does not rule out formation of this reflector as an earlier inherited feature, as it could have served as a weakness to reactivate in the crust during shortening.

The steep-to-shallow geometry of faults, rotated backlimbs, and presence of interpreted mid- to upper-crustal detachments is reminiscent of an imbricate fan geometry that is common in thin-skinned fold-thrust belts. In this interpretation, the Borrego fault would have been one of the first faults to exhibit motion, while east-stepping faults towards the front (east) would steepen previously formed faults. This mechanism can satisfactorily explain the fault geometries as constrained by surface and subsurface data. However, this imbricate fan kinematic model does not consider formation of Pennsylvanian–Permian Ancestral Rocky Mountain faults and later Laramide reactivation. Furthermore, Sutherland (1963) suggested that no rotation occurred on the Picuris-Pecos fault. Further analysis is necessary to test this idea of fault steepening during imbricate fan tectonism.

Thermal Framework

Thermochronology data show a clear spatial relationship, whereby AFT and AHe date populations are unique to each structural block (Figs. 3A–3C). Borrego block AHe and AFT dates are ~65–45 Ma. The range crest (Santa Fe block) samples are the oldest, exhibiting ~75–40 Ma AHe and AFT dates. AFT and AHe dates consistently young from the Santa Fe block to the east. The Pecos block exhibits ~65–20 Ma AHe and AFT dates, the Rincon block exhibits ~30–20 Ma AHe and AFT dates, while the Gallinas block exhibits ~25–10 Ma AHe and AFT dates. Frontal fold AHe dates are tightly constrained at 15–10 Ma. While all blocks show a fairly consistent population of date ranges, the Pecos block displays a broad range in AHe (Fig. 3B) and AFT (Fig. 3C) dates, and/or two populations of dates.

An interesting relationship is observed in the AFT lengths (Fig. 3d). All track lengths are generally 13–14 μm indicating moderate to rapid cooling, with longer tracks representing faster cooling (Gleadow et al., 1986). Borrego and Santa Fe

blocks exhibit broad track length standard deviations while other blocks are tightly constrained. The broad standard deviations in these blocks likely indicate slow continuous cooling (Gleadow et al., 1986). Pecos block track lengths are 13 μm, while Rincon and Gallinas blocks show 14 μm track lengths. The somewhat longer track lengths and short standard deviations indicate the quick cooling these blocks experienced at later dates, as shown by Landman (2016). There is an inverse relationship when considering the AFT dates with track lengths, in that the older AFT dates of the Pecos block exhibit the shortest tracks, while the progressively younger AFT dates show progressively longer track lengths in the Rincon and Gallinas blocks, respectively, with narrow standard deviations.

Apatite (U-Th)/He date-eU patterns (Fig. 3E) allow for interpretation of cooling history in that flat date-eU relationships likely indicate quick/fast cooling through the apatite partial retention zone and positive date-eU relationships likely indicate slower/prolonged cooling (Flowers et al., 2009). Dispersion in the AHe date-eU patterns is evident; some large date range dispersion at low (<10 ppm) eU may indicate U- and Th-rich grain coatings on analyzed grains (Murray et al., 2014). However, distinct populations for each structural block are evident. The spread of Borrego and Santa Fe block samples show a generally flat, possibly slightly positive, date-eU trend, while Santa Fe block samples show a second positive date-eU population. Pecos block samples show a positive date-eU trend and represent the largest span of eU for all samples. However, intermediate range eU data is absent for the Pecos block, and two possible trends with a shallow and steep positive date-eU relationship exist. Rincon block samples display a flat date-eU trend, but only moderate eU span. Gallinas block samples display ≤20 ppm eU that is insufficient to examine the date-eU trend. Frontal fold samples form a mostly flat date-eU trend.

Potential thermal histories can be tested against these date-eU patterns with forward models, as shown in Figure 4. Figure 5 shows the same data but for each structural block

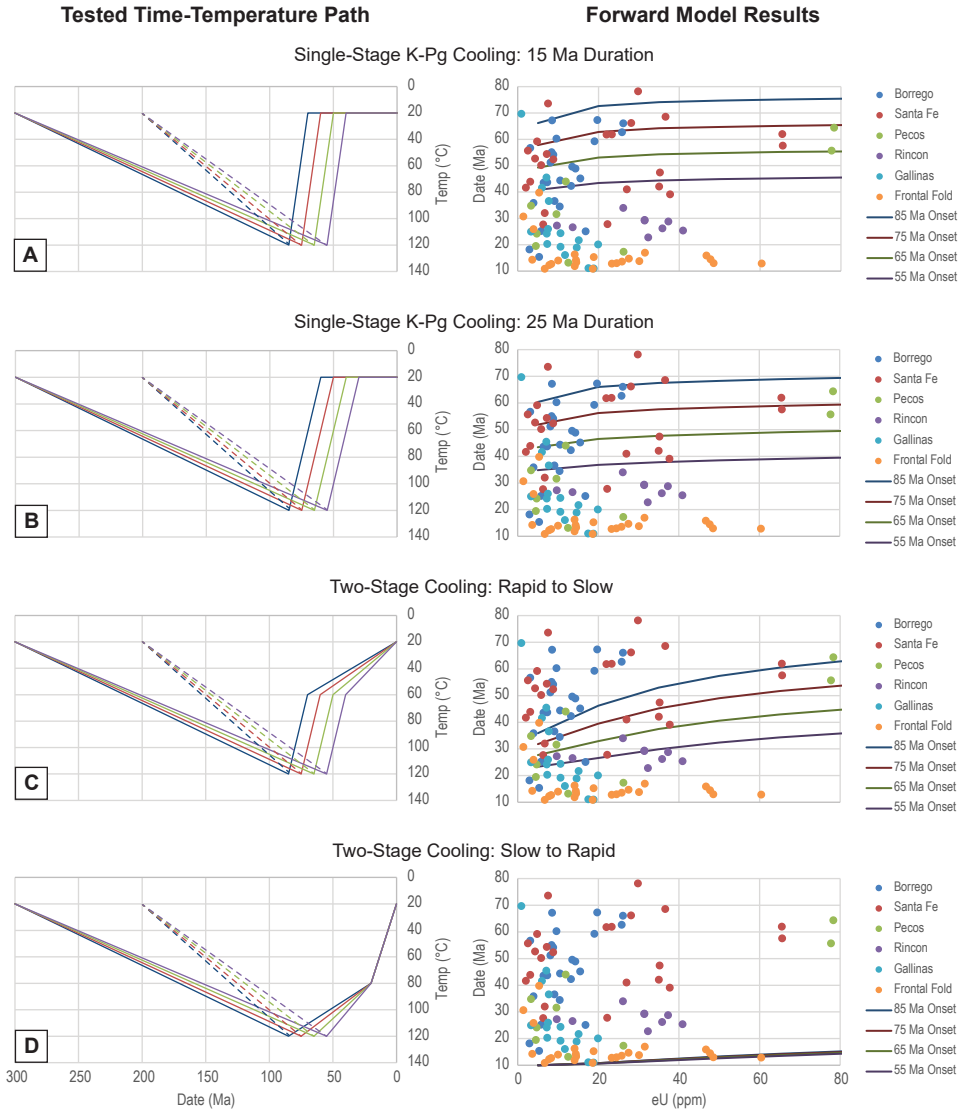

Figure 4. Forward model parameters (A–D left) and results for all AHe date-eU data by structural location (A–D right). Forward model parameters show Proterozoic-age samples started at 300 Ma; Triassic-age samples started at 200 Ma. Hypothetical paths are in 10 Ma increments from 85–55 Ma to test onset of cooling. Data dispersion at low eU across date ranges likely reflects U- and Th-rich grain boundary phases (Murray et al., 2016). Note distinct date-eU populations and forward model results for each structural block.

with the date-eU patterns for individual samples taken in those blocks and the preferred time-temperature model. Borrego and Santa Fe blocks can be fit by single-stage cooling that started ~75–65 Ma, although not all data from these blocks are fit by the single-stage model (Figs. 4A, 5A, and 5B). Younger AHe dates in the Santa Fe block correspond to samples at 300–800 m lower elevation (Fig. 5B; samples 81SF06, 81SF07). Pecos block samples can be fit either by two-stage rapid to slow cooling starting ~85 or 75 Ma (Fig. 4C and 5C), or by single-stage fast cooling at 65 Ma (Fig. 4A and 5C). Both models do not adequately explain low or high eU populations, suggesting a modified thermal history is necessary to explain this block's cooling history, but the slight positive date-eU trend likely requires a slower cooling history. The limited eU range for Rincon bench samples can be fit by two-stage initial cooling starting ~55 Ma followed by slow cooling to present (Figs. 4C and 5D). The <20 ppm eU span in Gallinas samples precludes forward modeling (Fig. 5E). Frontal fold data is tightly constrained and displays a broad eU span. These data can be fit by very slow cooling followed by quick exhumation from 20–0 Ma, but onset of cooling between 85 and 55 Ma cannot be resolved (Figs. 4D and 5E).

Despite data limitations and the oversimplified time-temperature models, some general interpretations can be made (Fig. 6). Trends appear to reflect earliest unroofing of the Borrego and Santa Fe blocks as part of the range crest at ~75 Ma. The positive date-eU trend in Santa Fe block samples represent lower elevation samples that cooled more slowly and/or were buried by range crest detritus. A similar model of range crest unroofing and forelimb/backlimb burial as recorded by AFT and AHe thermal histories was proposed by Thacker et al. (2021) for the Zuni arch in west-central New Mexico. The younger AFT and mean AHe dates for the Borrego block may also suggest burial, perhaps on the backlimb of the structure. The thermal history of the Pecos block is not well constrained but suggests either coeval exhumation with the Borrego and Santa Fe blocks or later ~65 Ma onset of cooling, perhaps due to burial. Dates, date-eU patterns, and forward models suggest that the Rincon and Gallinas blocks and frontal fold experienced deeper burial that prolonged cooling through the AHe partial retention zone. It is interpreted here that these patterns and younger dates reflect burial of these portions of the arch by detritus shed from the range crest while it was uplifting. The similarity of structures in each block requires they all formed during Laramide shortening; however, Late Cretaceous–Paleogene exhumation on the Gallinas block cannot be determined. Though limited, the results do provide partial support for an east-leading progression of exhumation from 75 Ma to ≤55 Ma.

The hypothetical time-temperature histories presented in the forward models are simplified and not intended to represent a final interpretation of the thermal histories within and across each block and the Sangre de Cristo arch. These time-temperature histories, however, can be used to infer distinctions in the blocks' thermal histories, and as such the general relationships of cooling provide a first-order interpretation of Sangre de Cristo arch tectonism. The thermal history forward models

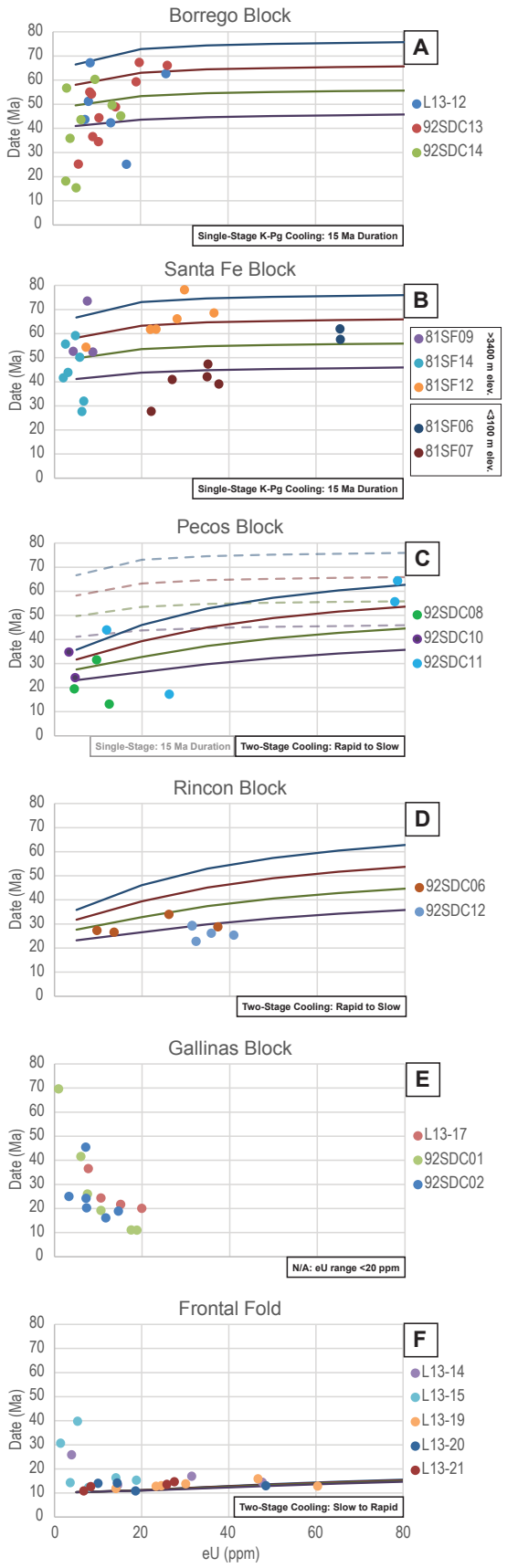

Figure 5. Forward model results for each block showing preferred time-temperature history. AHe date-eU patterns and forward model results. Data dispersion is evident, but distinct thermal histories are suggested across multiple samples in similar blocks.

represent a gross simplification for the purpose of analysis, and more detailed modeling is warranted. For example, a range of starting temperatures could account for the variability in preserved stratigraphic thicknesses/starting temperatures across the range (e.g., Proterozoic versus Triassic samples) at the start of Late Cretaceous exhumation as well as variable apatite annealing resistance (R_{mr0}). In addition, more nuanced analysis could involve multimethod (AFT and AHe) inverse modeling to explore a broader range of potential thermal histories. Additional sample and data collection would also be effective whereby samples could be collected on either side of major block-bounding faults. Care would need to be taken in this sampling to avoid structural complexities.

Tectonic Implications

The results and interpretations presented herein are leveraged to propose an imbricate fan fault geometry that sequentially stepped eastward. This model is geometrically and kinematically inconsistent with large-magnitude dextral slip (Cather, 1999; Cather et al., 2006) that accommodated a Colorado Plateau microplate (Karlstrom and Daniel, 1993). Geometrically, these models require high-angle strike-slip faults that cannot explain eastward-decreasing backlimb rotations and seismically imaged thrust fault geometries. Kinematically, these models do not explain the possibility of in sequence, east-leading strain. Limited dextral strain is permissible in a pervasive WSW–ENE shortening field superimposed on the S- to SSW-striking W- to WNW-dipping faults of the Sangre de Cristo arch. Thrust geometries are technically compatible with a transpressive positive flower structure, as proposed by Bauer and Ralser (1995). Similarly, the thermal histories could also suggest a flower structure. This would require that the Borrego and Picuris-Pecos faults are vertical strike-slip faults as opposed to the interpretations presented in Figure 2. The midcrustal character of these faults is not well constrained, and future work is warranted to test whether these fault geometries maintain a high-angle dip deeper into the midcrust, or if they shallow to the west as would be predicted by the interpretations presented herein.

The proposed imbricate fan geometry and east-leading in-sequence motion is more similar to Sevier-style, thin-skinned fold-thrust structures as opposed to Laramide-style thick-skinned structures. However, studies of Laramide structures support local-scale thin-skinned tectonism within the thick-skinned structure. In the Bighorn basin (Wyoming), the subsurface structure of the Elk Basin anticline has been modeled as a crystalline thin-skinned feature, where the subsurface fault is interpreted to flatten into a subhorizontal detachment within 3 km of the surface (Gray et al., 2019). These upper crustal faults were considered not to root down to deeper midcrustal (~30 km) detachments but rather acted to accommodate those deeper features. Geologic mapping by Geraghty (2013) in the Beartooth Mountains (Montana) shows strong evidence for lateral ramps and triangle zone deformation across a complex array of antithetic and synthetic (backthrust and forethrust) faults. These features are classic thin-skinned fold-thrust geometries but are important components of the thick-skinned, basement-involved deformation at the range front and in the subsurface of those Laramide structures.

At the regional scale, Parker and Pearson (2023) show convincing geometric and kinematic links between Sevier- and Laramide-style structures across Idaho to southwest Montana via midcrustal detachment. Mid- to upper-crustal detachments in north-central New Mexico Laramide structures have been previously considered, as Yin and Ingersoll (1997) suggested a midcrustal detachment that linked the Nacimiento and Sangre de Cristo arches. This idea is similar to midcrustal detachments suggested for Laramide structures in the northern Rocky Mountains (Erslev, 1993; Erslev et al., 2022). The results from this study are consistent with the midcrustal detachment model. Connection with the Nacimiento arch to the west is proposed (Fig. 7), showing a deeper depth to detachment than suggested by Yin and Ingersoll (1997) as well as the more complex network of interpreted imbricate fan faults within the Sangre de Cristo arch as presented (Fig. 2). A deeper detachment depth

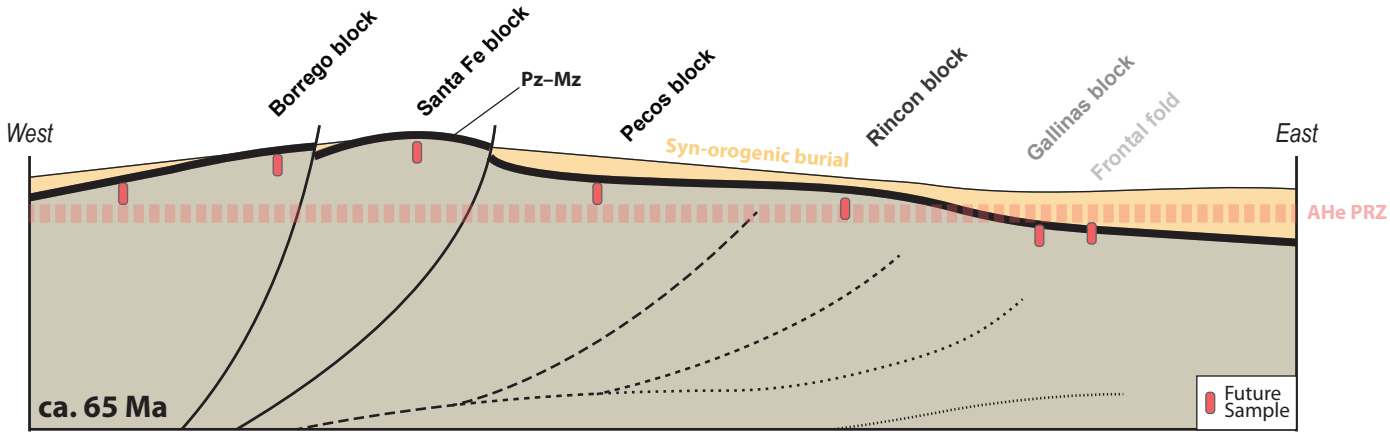

Figure 6. Hypothetical geometric and kinematic history of the Sangre de Cristo arch during Late Cretaceous–Paleogene Laramide-style tectonism. Geometric and thermochronologic data are used to interpret an east-stepping progression of thrust-driven exhumation, causing detritus shed from the range crest (Santa Fe and Borrego blocks) to bury the forelimb blocks (Pecos, Rincon, Gallinas) and the incipient frontal fold. AHe PRZ = apatite (U-Th)/He partial retention zone (90–40°C). Pz–Mz = Paleozoic through Mesozoic strata.

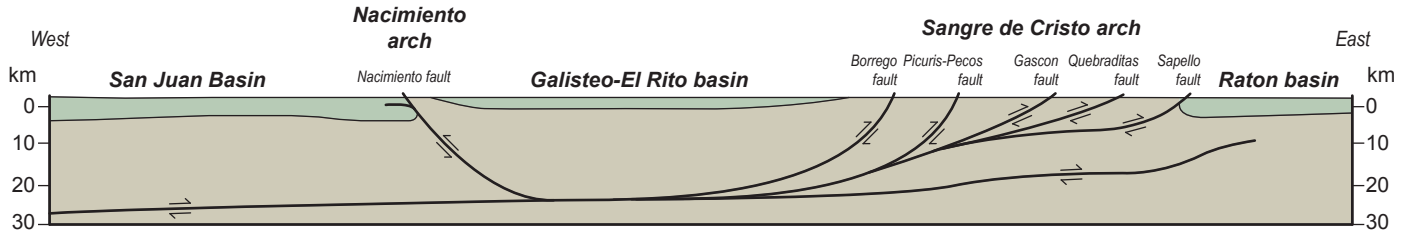

Figure 7. Proposed midcrustal detachment system connecting Sangre de Cristo and Nacimiento arches (Rocky Mountains) with the San Juan Basin (Colorado Plateau). Modified from Yin and Ingersoll (1997) to show complex thrust array beneath Sangre de Cristo arch. Brown = Proterozoic basement; green = Phanerozoic rocks.

is interpreted from the ~25 km deep seismic reflector shown in Magnani et al. (2005) interpreted herein as a Laramide detachment. These southern Rocky Mountain and Colorado Plateau-bounding Laramide features show stylistic similarities to northern Rocky Mountain Laramide structures. This geometric similarity may suggest a common causal mechanism for Laramide structures across the western interior USA portion of the Late Cretaceous–Paleogene North American Cordillera.

CONCLUSIONS

Structural and thermochronology data are used to interpret the geometric style and kinematic history of the southern Sangre de Cristo arch in north-central New Mexico. Two unbalanced trans-range cross sections constructed from surface geology and seismic data are used to present an imbricate fan style geometry for Sangre de Cristo arch faults. These faults transition from high-angle reverse faults on the west to progressively shallow thrust geometries on the east and are suggested to root into a midcrustal detachment. Thermochronology data show that the range crest (Santa Fe Range) exhumed first, and that blocks to the east likely exhumed later and/or were significantly buried by synorogenic detritus. It is interpreted that this cooling record represents east-leading in-sequence thrusts on the imbricate fan system.

These interpretations differ from previous suggestions for large-magnitude dextral transpression in north-central New Mexico (Chapin and Cather, 1981; Bauer and Ralser, 1995; Cather et al., 2006). Instead, horizontal shortening (e.g., Erslev, 2001; Fankhauser and Erslev, 2004) seems more viable given the fault geometries and timing of exhumation. Limited dextral motion is permitted, assuming a WSW–ENE-directed strain field acting on south-striking faults (Erslev, 2001; McDonald, 2003). It is further suggested that the proposed detachment level allows for connection of the Nacimiento and Sangre de Cristo arches, as shown by Yin and Ingersoll (1997). This midcrustal detachment model has been proposed for the Rocky Mountains (Erslev et al., 2022) and suggests a common tectonic mechanism for both the Colorado Plateau and Rocky Mountain provinces.

ACKNOWLEDGMENTS

Much appreciation is given to the field conference conveners, especially Kevin Hobbs, for their dedication to the conference and New Mexico Geological Society. The manuscript was improved by reviews from Jason Ricketts and Jeff Amato, with editorial handling by Kevin Hobbs.

REFERENCES

Bailey, J.M., Karlstrom, K.E., Reed, C.C., and Heizler, M.T., 2024, Structural geology of the Tierra Amarilla anticline, New Mexico: New Mexico Geological Society, Guidebook 74, p. 281–289. https://doi.org/10.56577/FFC-74.281

Baltz, E.H., 1972, Geologic map and cross sections of the Gallinas Creek area, Sangre de Cristo Mountains, San Miguel County, New Mexico: U.S. Geological Survey Miscellaneous Geologic Investigations, Map I-673, 2 sheets, scale 1:24,000. https://doi.org/10.3133/i673

Baltz, E.H., and Meyers, D.A., 1999, Stratigraphic framework of upper Paleozoic rocks, southeastern Sangre de Cristo Mountains, New Mexico, with a section on speculations and implications for regional interpretation of Ancestral Rocky Mountains paleotectonics: New Mexico Bureau of Mines and Mineral Resources Memoir 48, 273 p.

Bauer, P.W., and Ralser, S., 1995, The Picuris-Pecos fault—Repeatedly reactivated, from Proterozoic (?) to Neogene: New Mexico Geological Society, Guidebook 46, p. 111–115. https://doi.org/10.56577/FFC-46.111

Berg, R.R., 1962, Mountain flank thrusting in Rock Mountain foreland, Wyoming and Colorado: American Association of Petroleum Geologists Bulletin, v. 46, p. 2019–2032. https://doi.org/10.1306/BC743947-16BE-11D7-8645000102C1865D

Blackstone, D.L., 1980, Foreland deformation-Compression as a cause: Laramie, University of Wyoming, Contributions to Geology, v. 18, p. 83–100.

Bump, A.P., 2004, Three-dimensional Laramide deformation of the Colorado Plateau—Competing stresses from the Sevier thrust belt and the flat Farallon slab: Tectonics, v. 23. https://agupubs.onlinelibrary.wiley.com/doi/10.1029/2002TC001424

Bump, A.P., and Davis, G.H., 2003, Late Cretaceous–early Tertiary Laramide deformation of the northern Colorado Plateau, Utah and Colorado: Journal of Structural Geology, v. 25, p. 421–440. https://doi.org/10.1016/S0191-8141(02)00033-0

Cather, S.M., 1999, Implications of Jurassic, Cretaceous, and Paleozoic piercing lines for Laramide oblique-slip faulting in New Mexico and rotation of the Colorado Plateau: Geological Society of America Bulletin, v. 111, p. 849–868. https://doi.org/10.1130/0016-7606(1999)111<0849:IOJCAP>2.3.CO;2

Cather, S.M., 2004, Laramide orogeny in central and northern New Mexico and southern Colorado, *in* Mack, G.H., Giles, K.A., eds., The Geology of New Mexico—A Geologic History: New Mexico Geological Society Special Publication 11, p. 203–248.

Cather, S., Karlstrom, K., Timmons, J., and Heizler, M., 2006, Palinspastic reconstruction of Proterozoic basement-related aeromagnetic features in north-central New Mexico—Implications for Mesoproterozoic to late Cenozoic tectonism: Geosphere, v. 2, p. 299–323. https://doi.org/10.1130/GES00045.1

Chapin, C.E., and Cather, S.M., 1981, Eocene tectonics and sedimentation in the Colorado Plateau–Rocky Mountain area, *in* Dickinson, W.R., Payne, W.D., eds., Relations of Tectonics to Ore Deposits in the Southern Cordillera: Arizona Geological Society Digest, v. 14, p. 173–198.

Davis, G.H., and Bump, A.P., 2009, Structural geologic evolution of the Colorado Plateau, *in* Kay, S.M., Ramos, VA., Dickinson, W.R., eds., Backbone of the Americas—Shallow Subduction, Plateau Uplift, and Ridge and Terrane Collision: Geological Society of America Memoir 204, p. 99–124. https://doi.org/10.1130/2009.1204(05)

Erslev, E.A., 1993, Thrusts, back-thrusts and detachment of Rocky Mountain foreland arches, *in* Schmidt, C.J., Chase, R.B., Erslev, E.A., eds., Laramide Basement Deformation in the Rocky Mountain Foreland of the Western United States: Geological Society of America Special Paper 280, p. 339–358. https://doi.org/10.1130/SPE280-p339

Erslev, E.A., 2001, Multistage, multidirectional Tertiary shortening and compression in north-central New Mexico: Geological Society of America Bulletin, v. 113, p. 63–74. https://doi.org/10.1130/0016-7606(2001)113<0063:MMTSAC>2.0.CO;2

Erslev, E.A., and Koenig, N.V., 2009, Three-dimensional kinematics of Laramide, basement-involved Rocky Mountain deformation, USA—Insights from minor faults and GIS-enhanced structure maps, *in* Kay, S.M., Ramos, VA., Dickinson, W.R., eds., Backbone of the Americas: Shallow Subduction, Plateau Uplift, and Ridge and Terrane Collision: Geological Society of America Memoir 204, p. 125–150. https://doi.org/10.1130/2009.1204(05)

Erslev, E.A., Worthington, L.L., Anderson, M.L., and Miller, K.C., 2022, Laramide crustal detachment in the Rockies—Cordilleran shortening of fluid-weakened foreland crust: Rocky Mountain Geology, v. 57, p. 65–97. https://doi.org/10.24872/rmgjournal.57.2.65

Fankhauser, S.D., and Erslev, E.A., 2004, Unconformable and cross-cutting relationships indicate major Precambrian faulting on the Picuris-Pecos fault system, southern Sangre de Cristo Mountains, New Mexico: New Mexico Geological Society, Guidebook 55, p. 21–133. https://doi.org/10.56577/FFC-55.206

Flowers, R.M., Ketcham, R.A., Shuster, D.L., and Farley, K.A., 2009, Apatite (U-Th)/He thermochronometry using a radiation damage accumulation and annealing model: Geochimica et Cosmochimica Acta, v. 73, p. 2347–2365. https://doi.org/10.1016/j.gca.2009.01.015

Geraghty, E., 2013, Geologic map of the Stillwater Complex within the Beartooth Mountains front Laramide triangle zone, south-central Montana: Montana Bureau of Mines and Geology Open-File Report 645, 21 p., scale 1:48,000.

Gleadow, A.J.W., Duddy, I.R., Green, P.F., and Lovering, J.F., 1986, Confined fission track lengths in apatite—A diagnostic tool for thermal history analysis: Contributions to Mineralogy and Petrology, v. 94, p. 405–415.

Gray, G., Zhang, Z., and Barrios, A., 2019, Basement-involved, shallow detachment faulting in the Bighorn Basin, Wyoming and Montana: Journal of Structural Geology, v. 120, p. 80–86. https://doi.org/10.1016/j.jsg.2018.10.015

Karlstrom, K.E., and Daniel, C.G., 1993, Restoration of Laramide right-lateral strike-slip in northern New Mexico by using Proterozoic piercing points—Tectonic implications from the Proterozoic to the Cenozoic: Geology, v. 21, p. 1139–1142. https://doi.org/10.1130/0091-7613(1994)022%3C0862:ROLRLS%3E2.3.CO;2

Karlstrom, K.E., Lucas, S.G., Koning, D.J., Crumpler, L.S., Goff, F., Kelley, S.A., Reed, C.C., Iverson, N.A., and Crossey, L.J., 2024, Synopsis of the Nacimiento geologic nexus, New Mexico Geological Society, Guidebook 74, p. 105–126, https://doi.org/10.56577/FFC-74.105.

Karlstrom, K.E., Wilgus, J., Thacker, J.O., Schmandt, B., Coblentz, D., and Albonico, M., 2022, Tectonics of the Colorado Plateau and its margins: Annual Review of Earth and Planetary Sciences. https://doi.org/10.1146/annurev-earth-032320-111432

Kelley, S.A., and Duncan, I.J., 1986, Late Cretaceous to Middle Tertiary tectonic history of the northern Rio Grande rift, New Mexico: Journal of Geophysical Research Solid Earth, v. 91, p. 6246–6262. https://doi.org/10.1029/JB091iB06p06246

Kelley, S.A., Chapin, C.E., and Corrigan, J., 1992, Late Mesozoic to Cenozoic cooling histories of the flanks of the northern and central Rio Grande rift, Colorado and New Mexico: New Mexico Bureau of Mines and Mineral Resources Bulletin 145, 39 p. https://doi.org/10.58799/B-145

Ketcham, R.A., 2005, Forward and inverse modeling of low-temperature thermochronometry data: Reviews in Mineralogy and Geochemistry, v. 58, p. 275–314. https://doi.org/10.2138/rmg.2005.58.11

Koning, D.J., and Read, A.S., 2010, Geologic map of the southern Espanola Basin: New Mexico Bureau of Geology and Mineral Resources Open-file Report 531, scale 1:48,000. https://doi.org/10.58799/OFR-531

Landman, R.L., 2016, Thermochronologic investigations of Cenozoic unroofing and surface uplift in the southern Rocky Mountains and High Plains [Ph.D. dissertation]: Boulder, University of Colorado, 287 p.

Lisenbee, A.L., 2003, Geologic map of the Las Vegas NW quadrangle, San Miguel County, New Mexico: New Mexico Bureau of Geology and Mineral Resources Open-File Geologic Map 78, scale 1:24,000.

Magnani, M.B., Levander, A., Erslev, E.A., Bolay-Koenig, N., and Karlstrom, K.E., 2005, Listric thrust faulting in the Laramide front of north-central New Mexico guided by Precambrian basement anisotropies, *in* Karlstrom, K.E., Keller, G.R., eds., 2005, The Rocky Mountain Region—An Evolving Lithosphere—Tectonics, Geochemistry, and Geophysics: American Geophysical Union Geophysical Monograph Series, v. 154, p. 239–252.

McDonald, D.W., 2003, Fault reactivation: The Picuris-Pecos fault system of north-central New Mexico [Ph.D. dissertation]: Dallas, University Texas at Dallas, 539 p.

Murray, K.E., Orme, D.A., and Reiners, P.W., 2014, Effects of U-Th-rich grain boundary phases on apatite helium ages: Chemical Geology, v. 390, p. 135–151. http://dx.doi.org/10.1016/j.chemgeo.2014.09.023

Parker, S.D., and Pearson, D.M., 2023, A kinematic model linking the Sevier and Laramide belts in the Idaho-Montana fold-thrust belt, U.S. Cordillera: Geosphere, v. 19, p. 1565–1588. https://doi.org/10.1130/GES02649.1

Pollock, C.J., Stewart, K.G., Hibbard, J.P., Wallace, L., and Giral, R.A., 2004, Thrust wedge tectonics and strike-slip faulting in the Sierra Nacimiento, New Mexico: New Mexico Bureau of Geology and Mineral Resources Bulletin, v. 160, p. 97–111. https://doi.org/10.58799/B-160

Sales, J.K., 1968, Crustal mechanics of Cordilleran foreland deformation—A regional and scale-model approach: American Association of Petroleum Geologists Bulletin, v. 52, no. 8, p. 2016–2044.

Scholle, P.A., 2003, Geologic Map of New Mexico: New Mexico Bureau of Geology and Mineral Resources, scale 1:500,000. https://doi.org/10.58799/116894

Stearns, D.W., 1978, Faulting and forced folding in the Rocky Mountain foreland, *in* Matthews, III, V., ed., Laramide Folding Associated with Basement Block Faulting in the Western United States: Geological Society of America Memoir 151, p. 1–37 https://doi.org/10.1130/MEM151-p1

Stone, D.S., 1986, Geometry and kinematics of thrust-fold structures in central Rocky Mountain Foreland: American Association of Petroleum Geologists, Rocky Mountain Section Meeting.

Sutherland, P.K., 1963, Laramide orogeny, *in* Miller, J.P., Montgomery, A., Sutherland, P.K., eds., Geology of part of the Sangre de Cristo Mountains, New Mexico: New Mexico Bureau of Mines and Mineral Resources Memoir 11, p. 47–49.

Thacker, J.O., Karlstrom, K.E., Kelley, S.A., Kendall, J.J., and Crow, R.S., 2023, Late Cretaceous time-transgressive onset of Laramide arch exhumation and basin subsidence across northern Arizona—New Mexico, and the role of a dehydrating Farallon flat slab: Geological Society of America Bulletin, v.135, no. 1–2. https://doi.org/10.1130/B36245.1

Thacker, J.O., Kelley, S.A., and Karlstrom, K.E., 2021, Late Cretaceous–Recent low-temperature cooling history and tectonic analysis of the Zuni Mountains, west-central NM: Tectonics, v. 40. https://doi.org/10.1029/2020TC006643

Weil, A.B., and Yonkee, A., 2023, The Laramide orogeny—Current understanding of the structural style, timing, and spatial distribution of the classic foreland thick-skinned tectonic system, *in* Whitmeyer, S.J., Williams, M.L., Kellett, D.A., Tikoff, B., eds., Laurentia—Turning Points in the Evolution of a Continent: Geological Society of America Memoir 220, p. 707–771. https://doi.org/10.1130/2022.1220(33)

Wolf, R.A., Farley, K.A., and Kass, D.M., 1998, Modeling of the temperature sensitivity of the apatite (U-Th)/He thermochronometer: Chemical Geology, v. 148, p. 105–114. https://doi.org/10.1016/S0009-2541(98)00024-2

Woodward, L. A., 1976, Laramide deformation of Rocky Mountain foreland—Geometry and mechanics, tectonics and mineral resources of southwestern North America: Tectonics and Mineral Resources of Southwestern North America, New Mexico Geological Society Special Publication v. 6, p. 11–17. https://doi.org/10.56577/SP-6

Woodward, L.A., Hultgren, M.C., Crouse, D.L., and Merrick, M.A., 1992, Geometry of the Nacimiento-Gallina fault system, northern New Mexico, San Juan Basin, New Mexico Geological Society, Guidebook 43, p. 103–108. https://doi.org/10.56577/FFC-43.103

Yin, A., and Ingersoll, R.V., 1997, A model for evolution of Laramide axial basins in the southern Rocky Mountains, USA: International Geology Review, v. 39, p. 1113–1123. http://dx.doi.org/10.1080/00206819709465318

Yonkee, W.A., and Weil, A.B., 2015, Tectonic evolution of the Sevier and Laramide belts within the North American Cordillera orogenic system: Earth-Science Reviews, v. 150, p. 531–593. https://doi.org/10.1016/j.earscirev.2015.08.001